Distribution of the PAPR for Real-Valued OFDM Signals

Sulaiman A. Aburakhia
Mobile Systems International Consultancy "MSI Consultancy", KSA office , Riyadh, KSA
sulaiman.ahmed@msiuk.com
Ehab F. Badran
and Darwish A. Mohamed
Arab Academy for Science and Technology (AAST), Alexandria 21397, Egypt
ebadran@aast.edu, darwishm@eng.aast.edu

ABSTRACT

In the literature, the bounds of the peak to average power ratio (PAPR) are generalized to both complex-valued and real-valued orthogonal frequency division multiplexing (OFDM) signals. In fact, these bounds are accurately bounding the PAPR distribution of complex-valued OFDM signals only.

In this paper, we derive accurate PAPR bounds of real-valued OFDM signals and show that bounds of complex-valued OFDM signals cannot be generalized to the real-valued OFDM signals. Our analysis is based on the fact that a real-valued OFDM signal consists of a single random variable. Also a relation between the PAPR and number of subcarriers is established for both real-valued and complex-valued OFDM signals

Key Words: OFDM, PAPR, distribution of PAPR.

1. Introduction

Real-valued OFDM is used in high-speed modems for Digital Subscriber Line (DSL) applications [1]. The main drawback of OFDM signals is the high peak-to-average power ratio (PAPR), which could cause serious performance degradation in the presence of nonlinear power amplification. In literature, many techniques have been proposed to reduce PAPR [10 & reference therein] [11 & 12] and many approaches have been taken to analyze the distribution of PAPR [4-6] [13 & 14]. In this paper, we derive accurate and simple PAPR bounds of real-valued OFDM signals. Our analysis is based on the fact that a real-valued OFDM signal consists of a single random variable. Also we establish a relation between the PAPR and number of subcarriers for both real-valued and complex-valued OFDM signals.

The continuous-time OFDM signal can be expressed as [3]

$$s(t) = \sum_{k=0}^{N-1} S[k] e^{j2\pi f_k t}, \quad 0 \le t \le T_B \qquad (1)$$

where T_B is the OFDM symbol interval, N is the number of subcarriers, f_k is the center frequency of kth subcarrier, and $S[k] = a_k + jb_k$, is the complex data symbol sequence. The guard interval is ignored since it has no impact on the PAPR. Expressing $s(t)$ in terms of its real and imaginary parts yields

$$s(t) = s_I(t) + js_Q(t) == \sum_{k=0}^{N-1} \left(S[k]\cos 2\pi f_k t + jS[k]\sin 2\pi f_k t \right)$$

Therefore, the envelope of OFDM signal is

$$e(t) = |s(t)| = \sqrt{{s_I}^2(t) + {s_Q}^2(t)}$$

The peak of $s(t)$ is given by the maximum of its envelope $e(t)$, $\text{Peak}_{\max} = \max_{t\in[0,T_B]} |s(t)|$. Thus, the peak power is the maximum peak of the instantaneous power $|s(t)|^2$ is given by

$$P_{peak} = \max_{t\in[0,T_B]} |s(t)|^2 = \max_{t\in[0,T_B]} e^2(t)$$

and the average power of $s(t)$ is

$$P_{average} = \frac{1}{T_B}\int_0^{T_B} |s(t)|^2 dt = \frac{1}{T_B}\int_0^{T_B} e^2(t) dt$$

Thus, the peak-to-average power ratio is

$$\text{PAPR} = \frac{P_{peak}}{P_{average}} \qquad (2)$$

For N subcarriers with a unity power (e.g. subcarriers modulated with M-ary PSK, that is $s[k] = |s[k]| e^{j\phi_k}$, $|s[k]| = 1$), the average power is

$$P_{average} = \frac{1}{T_B}\int_0^{T_B} |s(t)|^2 dt = \frac{1}{T_B}\int_0^{T_B} \left| \sum_{k=0}^{N-1} e^{j(2\pi f_k t + \phi_k)} \right|^2 dt = N, \qquad (3)$$

and the maximum instantaneous signal power is N^2, which results when all subcarriers add coherently. So the PAPR can be as high as N, which is a theoretical maximum bound. If a multilevel constellation such as QAM is applied, this bound could be higher than N. However, the likelihood of all subcarriers to add coherently is extremely low. In [4], it was shown that for an OFDM system with 32 subcarriers, QPSK, and a symbol period of $T_B = 100\mu s$, the theoretical bound will be observed statistically only once in 3.7 million years. Therefore, it is better to describe

the PAPR of OFDM signals in terms of its statistical distribution. But first, the PAPR of discrete-time OFDM signals is formulated.

For the discrete-time OFDM signal,

$$s[n]=\sum_{k=0}^{N-1}S[k]e^{j\frac{2\pi nk}{N}}=s_I[n]+s_Q[n],\quad 0\le n\le N-1$$

where

$$s_I[n]=\sum_{k=0}^{N-1}\left(a_k\cos\left(\frac{2\pi nk}{N}\right)-b_k\sin\left(\frac{2\pi nk}{N}\right)\right),$$

$$s_Q[n]=\sum_{k=0}^{N-1}\left(a_k\sin\left(\frac{2\pi nk}{N}\right)+b_k\cos\left(\frac{2\pi nk}{N}\right)\right),$$

Thus, its envelope is $e[n]=|s[n]|=\sqrt{s_I^2[n]+s_Q^2[n]}$ and hence, the PAPR of the discrete-time signal is

$$\text{PAPR}=\frac{\max|s[n]|^2}{E\{|s[n]|^2\}} \qquad (4)$$

where $E\{\cdot\}$ denotes the mathematical expectation. Most of the PAPR reduction schemes including consider the discrete-time signal, where digital signal processing can be applied. However, the PAPR of the discrete-time signal provides a lower bound to the continuous-time one since peaks can occur during sampling time.

In [5], [6], the relationship between peak of the continuous signal and maximum of its sampled sequence was addressed, and a new bound for the peak of the continuous envelope of OFDM signal was proposed based on the maximum of its oversampled sequence. It was shown that an oversampling with a rate $L\ge 4$ is sufficient to tightly bound the peak of the continuous envelope. Thus, for an oversampling rate $L\ge 4$, the PAPR of continuous-time signal can be approximated very well by one of the discrete-time signal.

Oversampling with a rate of L can be achieved by inserting $(L-1)N$ zeros in the complex data sequence $S[k], 0\le n\le N-1$ prior to the *NL*-IDFT. Thus, the size of the IDFT/DFT is *NL*.

2. Statistical Analysis of PAPR

For a set of *M* complex symbols, there are M^N unique symbol sequences [4] and hence, M^N possible OFDM waveforms per OFDM symbol. Assuming that the data symbols $S[k], 0\le n\le N-1$ are statistically independent and identically distributed (i.i.d.) random variables (RVs), then, for a large number of subcarriers *N*, the central limit theorem [2] is applicable. Thus, for a large number of subcarriers *N*, real and imaginary parts of $s(t)$ approach the Gaussian distribution with a zero-mean and a common variance σ_s^2, with PDF given by

$$p_S(s)=\frac{1}{\sqrt{2\pi}\sigma_s}e^{-s^2/2\sigma_s^2} \qquad (5)$$

Figure 1 shows the simulated PDFs of real and imaginary parts of a randomly generated discrete-time OFDM signal with 64 subcarriers and oversampling rate $L=4$, the theoretical reference in (5) is plotted also. This figure demonstrates the accuracy of the Gaussian approximation to the real and imaginary part of OFDM signal.

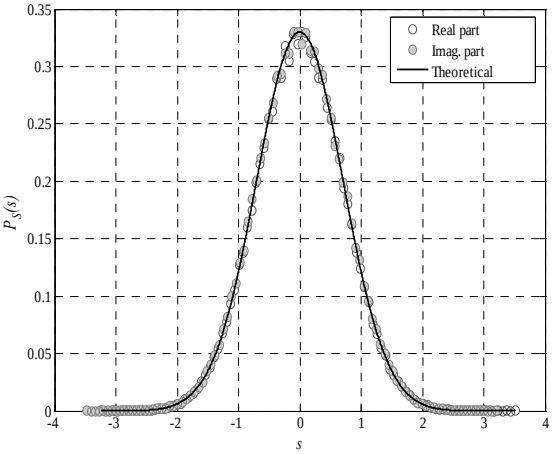

Figure 1: PDFs of complex-valued OFDM signal.

Since the real and imaginary parts are well modeled by zero-mean Gaussian distribution for a large number of subcarriers, the instantaneous signal power has a central chi-square distribution with two degrees of freedom, with a PDF given by

$$p_P(p)=\frac{1}{2\sigma_s^2}e^{-p/2\sigma_s^2},\qquad p\ge 0$$

It follows that the corresponding Cumulative Distribution Function (CDF) is

$$F_P(p)=\frac{1}{2\sigma_s^2}\int_0^p e^{-u/2\sigma_s^2}du=1-e^{-p/2\sigma_s^2},\quad p\ge 0 \qquad (6)$$

Thus, the probability that the normalized instantaneous signal power $P_{Normalized}=\frac{|s(t)|^2}{P_{average}}=\frac{p}{2\sigma_s^2}$, is above a given threshold p_o, is given by the complementary CDF (CCDF), i.e.,

$$P\left(P_{Normalized}>p_o\right)=\text{CCDF}=1-\text{CDF}=e^{-p_o} \qquad (7)$$

This CCDF is plotted in Figure 2 for different values of p_o.

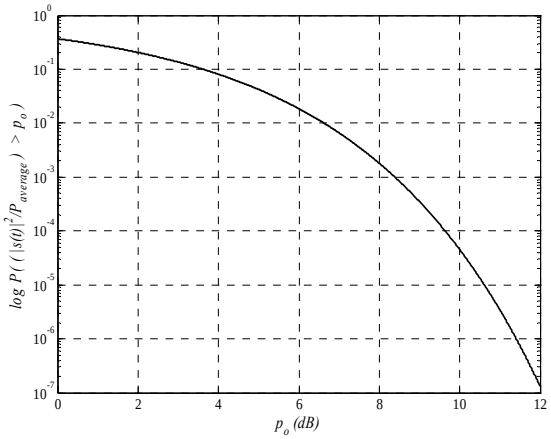

Figure 2: CCDF of the normalized instantaneous OFDM signal power.

As shown in Figure 2, large values of normalized instantaneous power have a very low probability to occur. However, since the PAPR depends on the signal envelope, it is better to consider the distribution of the OFDM signal envelope. Since the power has a central chi-square distribution with two degrees of freedom, the envelope is Rayleigh distributed with PDF given by

$$p_X(x) = \frac{x}{\sigma_s^2} e^{-x^2/2\sigma_s^2}, \quad x \geq 0 \qquad (8)$$

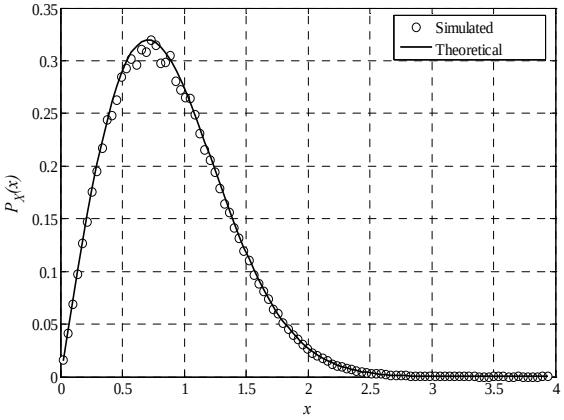

Figure 3: Simulated and theoretical envelope distributions of complex-valued OFDM signal.

Figure 3 shows the simulated and theoretical envelope distributions of complex-valued OFDM signal, as it shown, the envelope of complex-valued OFDM signal is very well modeled by the Rayleigh distribution. The corresponding CDF is

$$F_X(x) = \int_0^x \frac{u}{\sigma_s^2} e^{-u^2/2\sigma_s^2} du = 1 - e^{-x^2/2\sigma_s^2}, x \geq 0 \quad (9)$$

Thus, the probability that the PAPR = $\frac{\max|s(t)|^2}{P_{average}} = \frac{x^2}{2\sigma_s^2}$, is below or equal to a given threshold p_o for N subcarriers is

$$P(\text{PAPR} \leq p_o) = (\text{CDF})^N = \left(1 - e^{-p_o}\right)^N \qquad (10)$$

The probability that the PAPR is above p_o, is given by

$$P(\text{PAPR} > p_o) = 1 - (\text{CDF})^N = 1 - \left(1 - e^{-p_o}\right)^N, \quad (11)$$

which plotted in Figure 4 as a function of p_o for various numbers of subcarriers *N*.

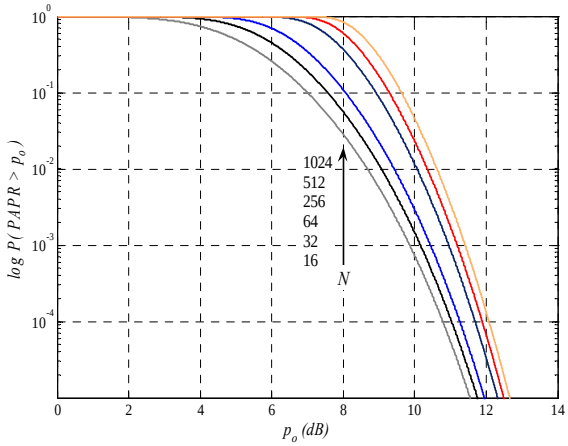

Figure 4: CCDF of the PAPR of OFDM signal for various numbers of subcarriers.

For discrete-time OFDM signal, (11) is valid when the samples are assumed to be mutually uncorrelated, i.e., each discrete time sample after the IDFT can be treated as independent of all other samples [7]. This assumption is true for non-oversampled OFDM signals [8]. An approximation to the PAPR distribution of oversampled signals was proposed in [9], by assuming that the distribution for N subcarriers with oversampling can be approximated by the distribution for αN subcarriers without oversampling, that is

$$P(\text{PAPR} > p_o) \approx 1 - \left(1 - e^{-p_o}\right)^{\alpha N}, \qquad (12)$$

with α larger than one, its value was determined by computer simulation to be 2.8. Thus, the effect of oversampling is approximated by adding a certain number of extra independent samples.

Figure 5 shows the simulated CCDF of complex-valued OFDM signals with 64 subcarriers, oversampling rate $L = 4$, and DQPSK modulation. The CCDF was obtained by randomly generating more than 10^5 OFDM symbols at each value of p_o and counting the number of symbols that their PAPR exceed this value, which is extremely a time consuming process. The approximation in (12) with $\alpha = 2.8$ is plotted along with the Theoretical reference in (11). As it shown, (12) accurately approximates the simulated distribution of oversampled signals. Simulation Results show that all generated symbols have a PAPR larger than 6 dB and less than 12 dB, while a PAPR larger than 11 dB occurred with a probability of 0.0004, i.e., only 40 symbols have a PAPR larger than 11 dB.

The CCDF of the PAPR is a useful metric to measure PAPR reduction capability (power efficiency) of various PAPR reduction schemes, since it provides a bound for the probability distribution of the PAPR.

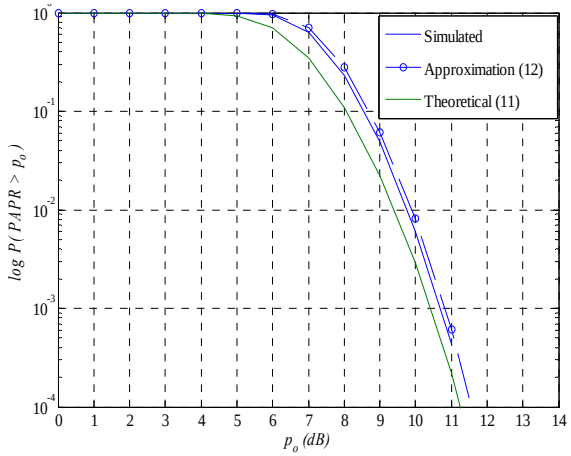

Figure 5: CCDF of complex-valued DQPSK-OFDM signal with 64 subcarriers and oversampling rate $L = 4$.

3. Distribution of the PAPR of Real-Valued OFDM Signals

In this Section, we derive accurate PAPR bounds of real-valued OFDM signals. Our analysis is based on the fact that a real-valued OFDM signal consists of a single random variable.

The real-valued OFDM signal after the Digital-to-Analog (D/A) converter can be expressed as

$$s(t) = 2\sum_{k=0}^{N-1}\left(a_k \cos 2\pi f_k t - b_k \sin 2\pi f_k t\right),\ 0 \le t \le T_B \quad (13)$$

and since $\sqrt{a_k^2 + b_k^2} = |S[k]|,\ \tan^{-1}\left(\frac{b_k}{a_k}\right) = \phi_k$, then, (13) can be rewritten as

$$s(t) = 2\sum_{k=0}^{N-1}\left[\,|S[k]|\cos\left(2\pi f_k t + \phi_k\right)\right],\ 0 \le t \le T_B \quad (14)$$

If all subcarriers are modulated by M-ary PSK, then $|S[k]| = 1$. Therefore the signal average power is

$$P_{average} = \frac{4}{T_B}\int_0^{T_B}\sum_{k=0}^{N-1}\left[\cos^2\left(2\pi f_k t + \phi_k\right)\right]dt = 2N, \quad (15)$$

and the maximum instantaneous signal power is $4N^2$, which results when all subcarriers add coherently. Therefore, the theoretical maximum bound of the PAPR of real-valued OFDM signals is $2N$, which twice the theoretical bound of complex-valued OFDM signals and hence, one can conclude that real-valued signals in general exhibit higher PAPR than complex-valued signals. From the central limit theorem, for a large number of subcarriers, the real-valued signal $s(t)$ will approach the Gaussian distribution with a zero-mean and variance σ_s^2, i.e., the signal is modeled as a real-valued Gaussian-distributed random variable. Therefore, its instantaneous power $|S(t)|^2$ has a central-chi-square with one degree of freedom with a PDF given by

$$p_P(p) = \frac{1}{\sqrt{2\pi p}\,\sigma_s}e^{-p/2\sigma_s^2},\quad p \ge 0$$

This implies that the signal envelope $\sqrt{|s(t)|^2}$ has a one-sided Gaussian distribution with a PDF given by

$$p_X(x) = \frac{\sqrt{2}}{\sqrt{\pi}\,\sigma_s}e^{-x^2/2\sigma_s^2},\quad x \ge 0 \qquad (16)$$

Thus, the envelope distribution of real-valued OFDM signals follows the one-sided Gaussian distribution rather than the Rayleigh distribution.

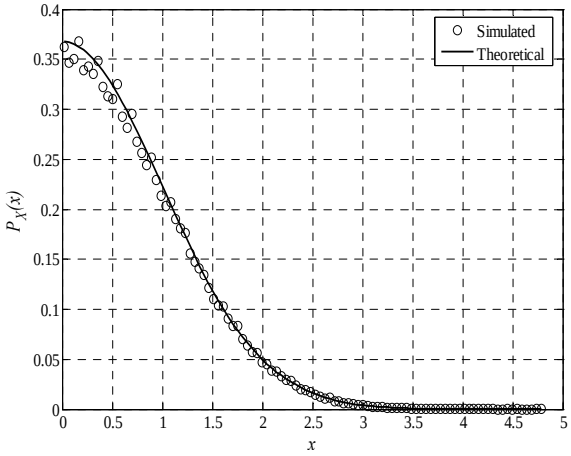

Figure 6: Simulated and theoretical envelope distributions of real-valued OFDM signal.

Figure 6 shows simulated distribution of a real-valued OFDM signal with 64 subcarriers, oversampling rate $L = 4,$ and QDPSK. The theoretical reference in (16) is plotted also. As it shown, envelope distribution is approximated very well by the one-sided Gaussian distribution. Its CDF thus is

$$F_X(x) = \frac{\sqrt{2}}{\sqrt{\pi}\,\sigma_s}\int_0^x e^{-u^2/2\sigma_s^2}du = erf\left(\sqrt{\frac{x^2}{\sigma_s^2}}\right), x \ge 0 \quad (17)$$

where $erf(x) = \frac{2}{\sqrt{\pi}}\int_0^x e^{-t^2/2}dt$ is the error function.

Thus, the probability that the PAPR of real-valued OFDM signal, which is $\text{PAPR} = \frac{\max|s(t)|^2}{P_{average}} = \frac{x^2}{\sigma_s^2}$, is below or equal to a given threshold p_o for N subcarriers is given by

$$P\left(\text{PAPR} \le p_o\right) = \left(\text{CDF}\right)^N = \left[erf\left(\sqrt{p_o}\right)\right]^N$$

The probability that the PAPR is above p_o, is given by the CCDF,

$$P\left(\text{PAPR} > p_o\right) = 1 - \left(\text{CDF}\right)^N = 1 - \left[erf\left(\sqrt{p_o}\right)\right]^N \quad (18)$$

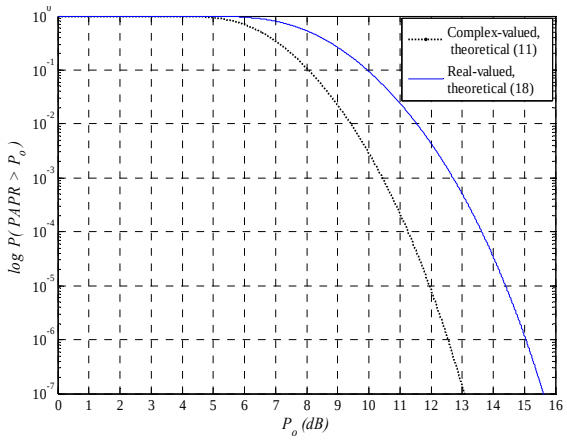

Figure 7: Theoretical CCDFs of real-valued and complex-valued OFDM signals with $N = 64$.

Figure 7 shows theoretical CCDFs of real-valued and complex-valued OFDM signals with $N = 64$. As it is shown Figure 7, the approximation in (11) provides inaccurate bound of real-valued OFDM signals. Furthermore, it is clear that real-valued signals exhibit higher PAPR since their theoretical maximum bound is twice that of complex-valued. Specifically, the probability that PAPR exceed 12 dB is 8×10^{-6} for complex-valued signals, while for real-valued signals this probability is 0.004, which is much higher. For oversampled real-valued OFDM signals, we suggest the same approximation approach that used in [9] for complex-valued, i.e. the effect of oversampling is approximated by adding a certain number larger than one of extra independent samples. Therefore, for oversampled real-valued OFDM signals, the CCDF can be approximated by

$$P\left(\text{PAPR} > p_o\right) = \text{CCDF} \approx 1 - \left[erf\left(\sqrt{p_o}\right)\right]^{\alpha N} \quad (19)$$

with α larger than one, its value was determined by computer simulation to be 3.5. Figure 8 shows simulated CCDFs of real-valued and complex-valued OFDM signals with 64 subcarriers, oversampling rate $L = 4$, and QDPSK modulation. Approximations in (12) and (19) are plotted along with the simulated data.

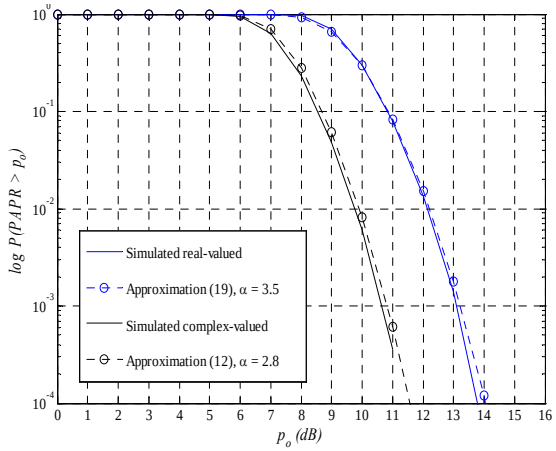

Figure 8: Simulated CCDFs of real-valued and complex-valued OFDM signals with 64 subcarriers, oversampling rate $L = 4$, and QDPSK modulation.

As it shown in Figure 8, simulation results demonstrate the accuracy of (19); it is tightly bounding the PAPR of real-valued OFDM signals. Furthermore, results confirm that real-valued signals are generally exhibiting higher PAPR than complex-valued signals. Specifically, among 100000 randomly generated complex-valued OFDM symbols, no symbol has a PAPR higher than 11 dB, while for real-valued signals, among the same number of random symbols, about 8244 symbols have a PAPR that is higher than 11 dB. An interesting observation is that at $p_o \geq 7$ dB, the PAPR of real-valued signals on the average is approximately 2 dB higher than that of complex-valued signals.

Figure 9 shows simulated and approximated CCDFs of real-valued OFDM signals with oversampling rate $L = 4$ and QDPSK modulation at various numbers of subcarriers. Results depict the accuracy of the approximation in (19). It is also observed that at given threshold p_o, the probability that the PAPR exceeds this threshold increases as N increases. Specifically, at $p_o = 12$ dB, the CCDF with N = 128 subcarriers is 0.03, while with N = 1024, the CCDF is 0.24.

In general, the PAPR grows as the number of subcarriers increases and can be as high as N for complex-valued signals and as high as $2N$ for real-valued signals, when all subcarriers add coherently, which is a theoretical maximum bound with a very low likelihood.

So far, we have derived an accurate bound for the PAPR distribution of oversampled real-valued OFDM signals. This bound (Equation (19)) has no closed form since it involves the error function, which cannot be determined analytically. Therefore, in order to obtain the CCDF of real-valued OFDM signals, numerical methods should be performed.

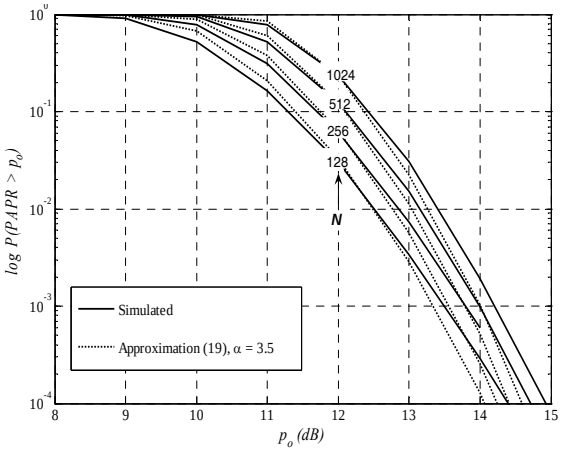

Figure 9: Simulated and approximated CCDFs of real-valued OFDM signals with oversampling rate $L = 4$ and QDPSK modulation at various numbers of subcarriers N.

However, since real-valued OFDM signals are generally exhibiting high PAPR, a closed-form approximation to (19) can be obtained based on the asymptotic series expansion of the complementary error function erfc, which is related to the erf function by the following relation

$$erf(x) = 1 - erfc(x), \tag{20}$$

where,

$$erfc(x) = \frac{2}{\sqrt{\pi}} \int_{x}^{\infty} e^{-t^2/2} dt$$

By assuming $x = \sqrt{p_o}$, and substituting (20) into (19) yields

$$P(\text{PAPR} > p_o) = \text{CCDF} = 1 - \left[1 - erfc\left(\sqrt{p_o}\right)\right]^{\alpha N} \tag{21}$$

For large values of $\sqrt{p_o}$, the complementary error function erfc may be approximated by the asymptotic series

$$erfc\left(\sqrt{p_o}\right) = \frac{e^{-p_o}}{\sqrt{p_o \pi}} \left(1 - \frac{1}{2p_o} + \frac{1 \cdot 3}{2^2 p_o^2} + \frac{1 \cdot 3 \cdot 5}{2^3 p_o^3} + ...\right) \tag{22}$$

Since OFDM signals are generally exhibiting high PAPR, that is $p_o >> 1$, then the first term in (22) is dominant and other terms can be neglected. Thus, (22) can be approximated in a closed form with a very low error as

$$erfc\left(\sqrt{p_o}\right) = \frac{e^{-p_o}}{\sqrt{p_o \pi}} \tag{23}$$

Substituting (23) into (21) leads a closed-form approximation to the bound of real-valued OFDM signals as

$$P(\text{PAPR} > p_o) = 1 - \left[1 - \left(\frac{e^{-p_o}}{\sqrt{p_o \pi}}\right)\right]^{\alpha N} \tag{24}$$

Figure 10 compares CCDF of the PAPR of real-valued OFDM signals to its closed-form approximation at various numbers of subcarriers *N*. As it seen, among all values of *N*, the approximation error is almost zero.

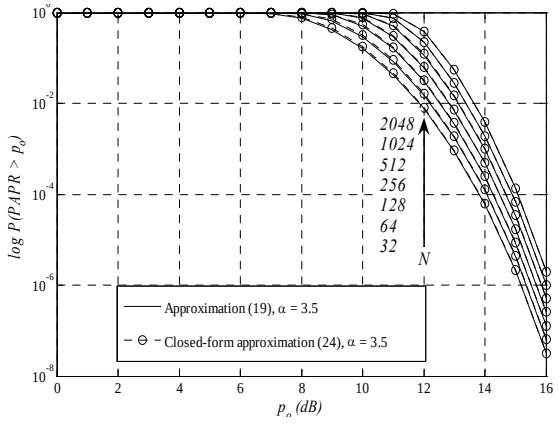

Figure 10: CCDF of the PAPR of real-valued OFDM signals and its closed-form approximation at various numbers of subcarriers *N*.

As mentioned earlier, the PAPR grows as the number of subcarriers increases. Thus, it seems that PAPR increases approximately linearly with the number of subcarriers. Practically, this places a tradeoff between PAPR and *N* in the design of OFDM systems. More specifically, in frequency selective fading channels that have relatively large multipath delays, it is desirable to employ large number of subcarriers in order to ensure that each subcarrier will experience relatively a flat fade, which on the other hand leads to high PAPR.

In the next section, we investigate the relationship between the PAPR and the number of subcarriers and see how the PAPR actually grows with the number of subcarriers.

4. The Relation between PAPR and Number of Subcarriers

Figure 11 shows the CCDF of the PAPR as a function of the number of subcarriers *N* for various values of p_o, it is obvious that for large values of *N*, CCDF is almost constant. Furthermore, at a given number of subcarriers *N*, CCDF decreases as p_o increases.

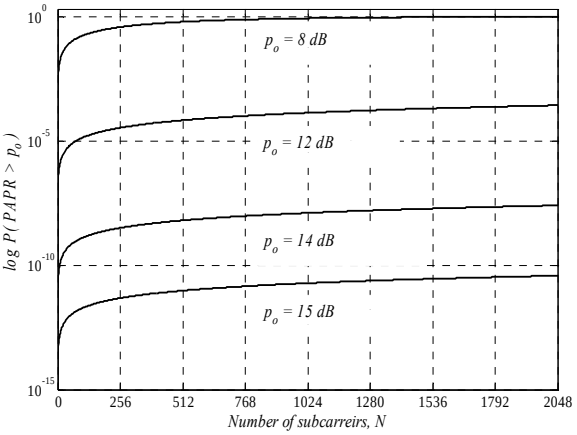

Figure 11: CCDF of the PAPR as a function of number of subcarriers *N* for various values of p_o .

From these observations, one can conclude that linear relationship between the PAPR and the number of subcarriers is true only for small number of subcarriers since the likelihood for all or most of the subcarriers to add coherently is relatively high. As the number of subcarriers increases, this likelihood decreases and can be neglected for large number of subcarriers. Nevertheless, it is more meaning full to address the variation of the PAPR with large number of subcarriers.

The relationship between the number of subcarriers *N* and PAPR can be established by recalling (11), since $e^{-p_o} << 1$, the second term in the right hand side can be approximated as

$\left(1-e^{-p_o}\right)^N \approx 1-Ne^{-p_o}$, thus,
$\rho = 1-\left(1-Ne^{-p_o}\right) = Ne^{-p_o}$. Solving for p_o yields

$$p_o = \ln\left(\frac{N}{\rho}\right) \tag{25}$$

ρ can be approximated by the probability of full coherent addition. For an M-ary PSK-OFDM system, there are M^N unique symbol sequences and hence, M^N possible OFDM waveforms per OFDM symbol, and at most M^2 patterns that yield the theoretical upper bound of PAPR [4]. Thus,

$$\rho \approx \frac{\mathrm{M}^2}{\mathrm{M}^N} = \mathrm{M}^{-(N-2)} = \frac{1}{\mathrm{M}^{N-2}} \approx \frac{1}{N}, \tag{26}$$

Substituting (26) into (25) yields

$$p_o = \ln\left(N^2\right) \tag{27}$$

Thus, for large number of subcarriers, the PAPR grows as a function of $\ln(N^2)$ rather than as of *N*. Figure 12 shows the simulated PAPR as a function of the number of subcarriers *N*, where all subcarriers are modulated with QDPSK and oversampled by a factor of 4. The simulation was performed by randomly generating one complex-valued OFDM symbol at each *N* and measuring its PAPR, the process was repeated several times to average the PAPR. The relationship in (27) is plotted along with the simulated data.

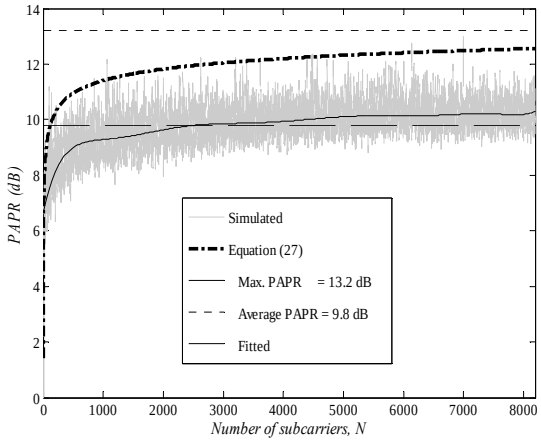

Figure 12: PAPR of oversampled complex-valued OFDM signals as a function of number of subcarriers *N*.

From simulation results, maximum PAPR was found to be around 13 dB, which occurred only in one symbols, i.e., with probability equals to $1/8192 = 1.22\times10^{-4}$. The average PAPR is 9.8 dB. The variance of PAPR values for $1 \le N \le 16$ is 2.9. For $16 \le N \le 8192$, The PAPR variance is 0.58, which means that for small number of subcarriers, the PAPR increases considerably with *N*, while for large values of *N*, the PAPR alternates around average value. This is demonstrated by Figure 13, which depicts the probability density of PAPR values among *N*.

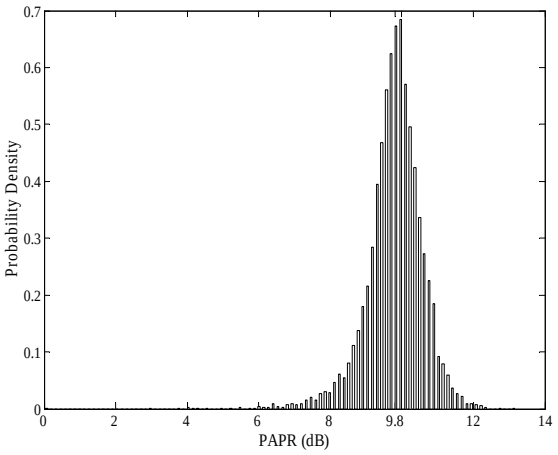

Figure 13: Probability density of PAPR values of complex-valued OFDM signals among *N*.

Regarding the relationship in (27), it is obvious that this relationship can be interpreted as an actual maximum bound of the PAPR, which leads to the conclusion that a tradeoff between PAPR and *N* does not exist actually.

A simulation with the same configurations was performed using real-valued OFDM signals, the results are shown in figure 14. From these results, the maximum PAPR was found to be around 14.99 dB, which occurred only in three symbols, while the average PAPR was 12.26 dB. For $1 \le N \le 16$ the PAPR variance is 3.52, while for $16 \le N \le 8192$, The PAPR variance is 0.64. The probability density of PAPR values among *N* is depicted in Figure 15.

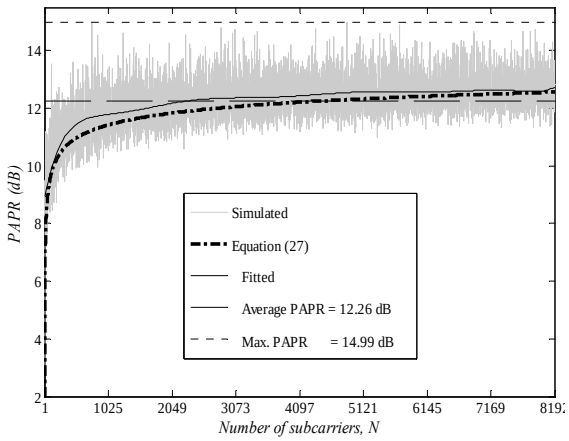

Figure 14: PAPR of oversampled real-valued OFDM signals as a function of number of subcarriers *N*.

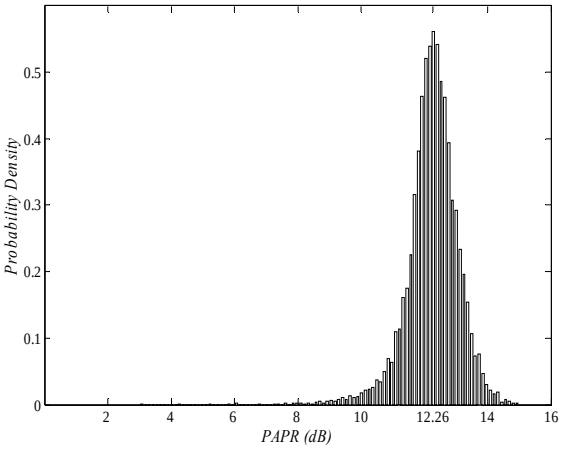

Figure 15: Probability density of PAPR values of real-valued OFDM signals among *N*.

Comparing results of Figure 14 to those of Figure 12, leads to two important observations. First, the average PAPR of real-valued signals is about 2 dB more than that of complex-valued. Therefore, for a given PAPR reduction scheme to be adopted for real-valued OFDM signals, a margin of 2 dB should be inserted. Second, the relationship in (53) now describes the actual behavior of PAPR of real-valued signals, in other words, the PAPR of real-valued OFDM signals provide an actual maximum bound to that of complex-valued.

5. Conclusion

In section 3 of this paper, accurate PAPR bounds for real-valued OFDM signals have been driven. It has been demonstrated that the bounds of complex valued OFDM signal cannot be used with real-valued ones. A relation between the PAPR and number of subcarrier is established for both real-valued and complex valued OFDM signals in section 4.

References:

[1] J. S. Chow, J. C. Tu, and J. M. Cioffi, "A Discrete multitone transceiver system for HDSL applications," IEEE J. Select. Areas Commun., vol. 9, pp. 895-908, Aug. 1991.

[2] Athanasios Papoulis, *Probability, Random Variables, and Stochastic Processes,* 3rd ed. Boston, MA: McGraw-Hill, 1991.

[3] John G. Proakis, *Digital Communications*, 4th ed. McGraw-Hill, 2001.

[4] Hideki Ochiai and Hideki Imai, "On the Distribution of the Peak-to-Average Power Ratio in OFDM Signals," IEEE Trans. Commun., vol. 49, no. 2, pp. 282-289, Feb. 2001.

[5] M. Sharif and B. H. Khalaj, "Peak to mean envelope power ratio of oversampled OFDM signals: an analytical approach," in Proc. IEEE Int. Commun. Conf., Helsinki, Finland, vol. 5, pp. 1476-1480, June 2001.

[6] M. Sharif, M. G. Alkhansari, and B. H. Khalaj, "New results on the peak power of OFDM signals based on oversampling," in Proc. IEEE Int. Commun. Conf., Helsinki, Finland, vol. 2, pp. 866-871, Apr. 2002.

[7] D. Brillinger, *Time Series Data Analysis and Theory*, Philadelphia, PA: SIAM, 2001.

[8] Richard Van Nee and Ramjee Prasad, *OFDM for Wireless Multimedia Communications,* Boston, Artech House, 2000.

[9] Richard Van Nee, and Arnout de Wild, "Reducing the peak-to-average power ratio of OFDM," in Proc. 1998 IEEE Veh. Technol. Conf. (VTC '98), Ottawa, vol. 3, pp. 2072-2076, 1998.

[10] C. Schurgers and M. Srivastava, "A systematic approach to peak-to-average power ratio in OFDM," in Proc. SPIE, Vol. 4474, 2001, pp. 454 - 464.

[11]H. Ochiai and H. Imai, "Peak-Power Reduction schemes in OFDM systems : a review", in Proc. Int. Symposium on Wireless Personal Multimedia Commun., Yokosuka Research Park, pp. 247-252, Nov. 1998..

[12] S. H. Han and J. H. Lee, "An overview of peak-to-average power ratio reduction techniques for multicarrier transmission", IEEE Wireless Commun., vol. 12, pp.56-65, April, 2005.

[13] Hua Yu Min Chen Gang Wei, "Distribution of PAR in DMT systems", IEE Electr. Lett., vol. 39, pp. 799- 801, May 2003.

[14] Niklas Andgart, Per O¨ dling, Albin Johansson, and Per Ola Bo¨ rjesson, "Designing Tone Reservation PAR Reduction", EURASIP J. on Applied Signal Processing vol. 2006, pp. 1-14, 2006.